IEEE Access
Multidisciplinary | Rapid Review | Open Access Journal

Received May 4, 2020, accepted May 21, 2020, date of publication May 25, 2020, date of current version June 5, 2020.

Digital Object Identifier 10.1109/ACCESS.2020.2997378

A Chaos Disturbed Beetle Antennae Search Algorithm for a Multiobjective Distribution Network Reconfiguration Considering the Variation of Load and DG

JIE WANG, WEIQING WANG, ZHI YUAN, HAIYUN WANG, AND JIAHUI WU

Engineering Research Center of Education Ministry for Renewable Energy Power Generation and Grid-connected Control, Xinjiang University, Urumqi 830047, China

Corresponding author: Weiqing Wang (wangwq666@gmail.com)

This work was supported in part by the National Natural Science Foundation of China under Grant 51667020 and Grant 51666017, in part by the Autonomous Region Government under Grant 2018D04005, in part by the Xinjiang Autonomous Region under Grant XJEDU2019I009, and in part by the Ministry of Education under Grant IRT-16R63.

ABSTRACT As the distributed generation (DG) in a power supply and the user load demand constantly change in an actual distribution network, multiobjective optimal network reconfiguration considering variations in load and DG has become a major concern, which is important and required to make system operations safe and economical. The aim is to minimize the sum of the active power loss, the sum of the load balancing index and the sum of the maximum node voltage deviation index simultaneously during the reconfiguration period. Here, this article proposes a new Chaos Disturbed Beetle Antennae Search (CDBAS) algorithm to reduce the computational time and solve the multiobjective optimal problem of network reconfiguration. To adopt the Chaos Disturbed Beetle Antennae Search algorithm for solving this multiobjective problem, grey target decision-making technology is used to rank the beetles. Additionally, to the enhance the system static voltage stability and voltage quality, a grey target decision-making model is established to achieve a layer relationship between each index and the switching operation index. The plausibility and effectiveness of the presented methodology is verified on the modified IEEE 33, 69 and 118-Bus Test Radial Distribution Network. Finally, compared with other research methods in the literature, the CDBAS algorithm outperforms other algorithms and produces a quality decision solution.

INDEX TERMS Distribution system, load and distributed generation variation, multiobjective optimization, grey target decision-making, CDBAS algorithm.

I. INTRODUCTION

The combination of residential, commercial and industrial loads creates differences and time variabilities on the feeders of a distribution network, which make the operational control of the distribution network very complicated and pose challenges for system safety and economy as well as user comfort. Wind power and photovoltaics are increasingly developed sustainable clean energy sources that have attracted increasing interest in the last decade due to increasing power demands and the increasing consumption of fossil fuels. Thus, distributed generation (DG) into distribution networks has become popular considering the technical advantages of DG units in reducing network losses, balancing demand overloads, improving the node voltage level and absorbing renewable energy [1]. With the active management of advanced metering facilities and information communication technology in the network topology structure and distributed power supply, a network reconstruction with different factors, which can deal with the time variabilities of load and DG more flexibly, is viable.

Distribution network reconfiguration can also be defined as the status of changing switches to improve system operation. For example, a dispatcher obtains the optimal network topology by opening a closed section switch and then closing an open tie switch under the condition of satisfying constraints such as voltage and current limits, radial structures and power flows. To date, many researchers have investigated network

The associate editor coordinating the review of this manuscript and approving it for publication was Alexander Micallef.

reconfiguration with classic techniques and heuristics for single and multiple objectives with the aim of achieving a safe and reliable operation point of the distribution system [2]–[4].

Many studies have exploited hybrid algorithms based on previously cited researchers who proposed methods for multiobjective distribution system reconfiguration in a structure, as in [5], [6], and other studies have considered the correlation among objectives by the grey correlation method in evolutionary programming and its role in optimizing particles by integrating the objectives. Additionally, some studies have focused on providing the multiobjective problem of network reconfiguration with different techniques, such as fuzzy evaluation theory [8]–[10] and cloud theory [11], and all of these approaches can obtain ideal solutions with better objectives [12], [13]. These methods, which are subject to uncertainty theory, can improve the quality of the solutions, especially for traditional distribution systems, but they cannot achieve the optimal variability of load and DG for a distribution network.

In the literature, studies have examined the concept of optimal multiobjective reconfiguration with the variability of load and DG in the distribution system. The authors of [14] used a multiobjective reconfiguration evolutionary technique of a distribution feeder system with wind turbines and fuel cells to consider the variability of wind power output and load demand for the benefit of minimum losses and better economic costs. Additionally, [15], [16] had the same objective and considered the same distributed generation with different techniques but did not address the calculation time, and other authors have studied multiobjective reconfiguration from the aspect of the convergence rate based on the security index to achieve the best result where the number of iterations is an obstacle [17], [18]. Some of these studies did not consider load time variation [19], [20]. Then, the author of [21] established a bi-objective dynamic reconfiguration model that considers the optimal equilibrium relationship between loss reduction and switching action reduction to obtain the best solution, but the load balance and voltage quality were not considered.

All of the abovementioned papers demonstrate the multiobjective reconfiguration of distribution networks based on specific types of metaheuristic and some new techniques to achieve different objectives, which are converted to a single objective aiming to find a trade-off solution by the most common methods, such as the compromise model [22]–[25], the entropy method [26], and the analytic hierarchy process [21], [27], without considering the mutual constraints among the objectives. However, the simple multiobjective traditional methods are no longer applicable for an automated distribution system with multiple conflicting objectives for scheduling known optimized solutions simultaneously. To solve the trade-off solution problem, we use the grey target decision-making technique to establish a layer relationship between active power loss, the load balancing index and the maximum node voltage deviation index with the number of switching operation indices for optimal multiobjective network reconfiguration. Here, this paper uses a Beetle Antennae Search algorithm based on Chaotic Disturbance (CDBAS) to solve the problem of multiobjective optimal network reconfiguration to reduce the calculation time through the individual advantage of the beetle. The Beetle Antennae Search, first designed and developed by Jiang X Y, is a bioinspired intelligent optimization algorithm, which was inspired by the foraging principle of beetles [28], [29]. The original Beetle Antennae Search (BAS) algorithm often converges slowly, has low accuracy and searches for local optima easily. To avoid the above shortcomings, the original BAS combined with the chaotic disturbance mechanism (CDBAS) approach is proposed. A grey target decision-making technique [30] is adapted to the CDBAS algorithm for determining the order of the beetles with the solution problem of multiobjective optimization network reconstruction. Finally, we simulate the proposed methodology in the modified IEEE 33-bus Distribution Network System and subsequently analyse the optimization results, which verify the feasibility and validity of the method. In addition, compared with other methods in the literature, the proposed methodology can achieve better for solution quality.

The main contributions of this paper are as follows:

- We propose a new CDBAS method for a multiobjective optimization network reconstruction model, which enhances a reduction in calculation time.
- We propose a grey target decision-making technique for the order of beetles, which can achieve the actual solution required by personnel.
- To enhance the system voltage quality and stable system operation, we use the grey target decision-making method to achieve the layer relationship between each index and the number of switching operation indexes.
- To ensure safe and economical system operation, we carry out 5 reconfigurations according to the load curve over 24 hours.

The logical framework of this work is as follows. Section II provides the load and DG curves. Section III introduces the objective functions and the constraint. Section IV describes the calculation process of the grey target decision-making method. Section V explains the CDBAS algorithm. Section VI demonstrates the simplification and encoding of topology based on a basic loop. Section VII shows the test results of 8 benchmark functions from the CDBAS algorithm, the results from the modified 33, 69 and 118-bus system and a comparison with other methods. Finally, Section VIII presents the paper's conclusions.

II. LOAD AND DG PATTERN

The variation in the DG power supply and user load demand during a typical day has a significant effect on the safe and economical operation of a power system.

A. LOAD DEMAND PATTERN

Since users have relatively fixed demand proportion curves during a typical day in the same region and season, the loads

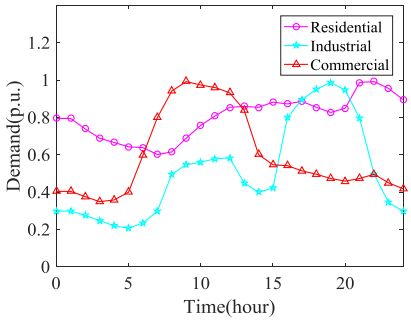

FIGURE 1. Load duration curves of each type for 24 hours.

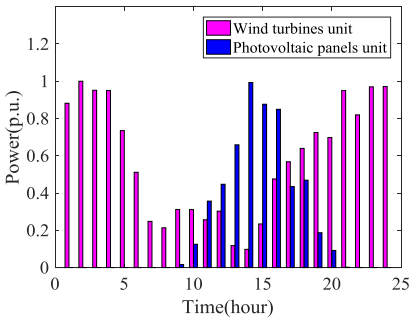

FIGURE 2. Wind and photovoltaic output curves.

can be described by demand proportion curves per day [31]. In general, the load obtained by daily loads in summer in a certain region involves three categories: residential, industrial and commercial, as shown in Fig. 1. The load curves of each node are different, and the daily load curve P_{Li} of node 'i' can be described as

$$P_{Li} = \sum_{s \in S} P_{Ni}\theta_{si}\delta_s \tag{1}$$

where S = {s|1,2,3} is the set of load types; $s = 1$ is residential, s = 2 is industrial, and s = 3 is commercial; P_{Ni} is the rated power of load node 'i'; and θ_{si} represents the ratio of load type 's' in the total load of node 'i'. δ_s represents the demand curves of load type 's'.

B. TYPICAL DG OUTPUT

The duration curves of wind power and photovoltaic power generation are shown by curves for a day in summer in a certain region in Fig. 2. The load data of each node and the DG output can be obtained by prediction techniques in the actual operation of the system.

III. PROBLEM FORMULATION

A. OBJECTIVE FUNCTION

Considering the optimization objective of network reconfiguration from the aspects of economy, voltage quality and load balance is practical. Here, the sum of the active power loss, the sum of the load balancing index and the sum of maximum node voltage deviation are used to test the performance for the distribution system during hourly or every few hours of reconfiguration.

1) POWER LOSS INDEX

The calculation formula of active power loss for a distribution system is described as

$$f_1 = \min \sum_{T=1}^{TL} \sum_{m=1}^{M} D_m R_m \frac{P_m^2 + Q_m^2}{V_m^2} \tag{2}$$

where P_m represents the active power of the mth branch, Q_m represents the reactive power of the mth branch, R_m represents the resistance of the mth branch, V_m represents the initial voltage of the mth branch, D_m is the binary value, D_m represents the closed switch status in the mth branch when $D_m = 1$, D_m is the opening switch status for the ith branch when $D_m = 0$, M represents the number of branches, and TL represents the time length.

2) LOAD BALANCING INDEX

Load balancing requires the transfer of the negative load on the heavy line to the light line for network reconstruction, the load-balancing index is calculated as

$$f_2 = \min \sum_{T=1}^{TL} \sum_{m=1}^{M} D_i \frac{\sqrt{P_m^2 + Q_m^2}}{S_m^{\max}} \tag{3}$$

where S_m^{max} represents the maximum complex power of branch 'm'.

3) VOLTAGE DEVIATION INDEX

$$f_3 = \min \sum_{T=1}^{TL} \max \left(\frac{V_1 - V_{1r}}{V_{1r}}, \cdots, \frac{V_i - V_{ir}}{V_{ir}}, \cdots, \frac{V_N - V_{Nr}}{V_{Nr}} \right) \tag{4}$$

where V_i represents the virtual voltage of the ith node, V_{ir} represents the rated voltage of the ith node, and N represents the total number of nodes.

B. OPERATIONAL CONSTRAINTS

1) NETWORK POWER FLOW CONSTRAINT

$$\begin{cases} P_i + P_{DGi} - P_{Li} = V_i \sum_{j=1}^{N} U_j (G_{ij} \cos\theta_{ij} + B_{ij} \sin\theta_{ij}) \\ Q_i + Q_{DGi} - Q_{Li} = V_i \sum_{j=1}^{N} U_j (G_{ij} \sin\theta_{ij} - B_{ij} \cos\theta_{ij}) \end{cases} \tag{5}$$

where P_{DGi} represents the active power of the DG connected to the ith node.

2) NETWORK NODES VOLTAGE LIMITS

$$V_i^{\min} \le V_i \le V_i^{\max} \tag{6}$$

where V_i^{min} and V_i^{max} are the allowable minimum and maximum values of the voltage at node i, respectively.

3) NETWORK LINE CAPACITY LIMITS

$$S_k \le S_k^{\max} \tag{7}$$

where S_i^{max} represents the allowable maximum capacity of branch 'k'.

4) RADIAL NETWORK CONSTRAINT

The network structure should meet radial topological constraints.

IV. GREY TARGET DECISION-MAKING MODEL

Because of the conflicting indexes, in this study, we use a grey target decision-making technique to solve the multiobjective problem to find the best reconfiguration solution. The optimization solution decision model is established by the grey target decision-making technique [30] considering the relationship between each index and the number of switching operation indexes.

Here, we define decision scheme set $S = \{S_1, S_2, \cdots, S_i, \cdots, S_n\}$, which is obtained by the CDBAS method, so switching operation index f_D is modeled as follows:

$$f_D = \sum_{T=1}^{TL} \sum_{j=1}^{N} 0.5 \left(D_{j,i+1} \oplus D_{j,i} + D_{j,i} \oplus D_{j,i-1}\right), \quad i = 0, 1, 2, 3 \tag{8}$$

where D_{ji} is the status of switch 'j' of reconfiguration scheme S_i, $D_{j,i+1}$ and $D_{j,i-1}$ are the statuses of switch 'j' for the other two reconfiguration schemes S_i, and f_D is the switch operation index of reconfiguration scheme 'i'.

Additionally, the grey target decision-making technique can be defined as finding the shortest distance between the solution of the candidate scheme set and the ideal solution, which is calculated as the decision value determined by the objective function. First, the effect sample matrix $T = [t_{ij}]_{n\times m}$ is formed, and the defined factor Z_j is calculated by the effect value determined for each index.

$$t_{ij} = \omega_1 f_{ij} + \omega_2 f_D \tag{9}$$

where t_{ij}(i = 1, 2, $\cdots$, n; j = 1, 2, $\cdots$, m) is the effect value of decision scheme S_i with respect to objective j. f_{ij} is the evaluation index of scheme S_i with respect to objective 'j'. $\omega_i(where\ i = 1, 2)$ is calculated by the entropy method [26].

$$z_j = \frac{1}{n}\sum_{i=1}^{n} t_{ij}, \quad j = 1, 2, \cdots, m \tag{10}$$

Then, the decision matrix $R = [r_{ij}]_{n\times m}$ is formed according to decision values (11), (12), and (13) with the benefit objective function, cost objective function, and interval objective function.

$$r_{ij} = \frac{(t_{ij} - z_j)}{\max\left\{\max\limits_{1\le i\le n}\{t_{ij}\} - z_j, z_j - \min\limits_{1\le i\le n}\{t_{ij}\}\right\}} \tag{11}$$

where r_{ij} represents the decision value when the objective function is defined as the benefit type index.

$$r_{ij} = \frac{(z_j - t_{ij})}{\max\left\{\max\limits_{1\le i\le n}\{t_{ij}\} - z_j, z_j - \min\limits_{1\le i\le n}\{t_{ij}\}\right\}} \tag{12}$$

where r_{ij} represents the decision value when the objective function is defined as the cost type index.

$$r_{ij} = \begin{cases} \dfrac{2t_{ij} - a - \min\limits_{1\le i\le n}\{t_{ij}\}}{a - \min\limits_{1\le i\le n}\{t_{ij}\}}, & t_{ij} < a \\ 1, & a \le t_{ij} \le b \\ \dfrac{2t_{ij} - b - \min\limits_{1\le i\le n}\{t_{ij}\}}{\min\limits_{1\le i\le n}\{t_{ij}\} - b} & t_{ij} > b \end{cases} \tag{13}$$

where $r_{ij} \in [-1, 1]$ represents the decision value when the objective function is defined as the interval [a,b] index.

However, we define the decision vector to be $r^0 = \{r_1^0, r_2^0, \cdots, r_m^0\}$, that is, the centre of the grey target, corresponding to the ideal solution S^0, where $r_j^0 = max\{r_{ij}|1 < i < n\}, j = 1, 2, \cdots, m$.

According to the grey target decision-making definition, the closer the target centre moment of solution S_i is to ideal solution S_0, the better the solution S_i is, and the distance between solution S_i and ideal solution S_0 is expressed as

$$d_i = \left|r_i - r^0\right| = \sqrt{\sum_{j=1}^{m} \gamma_j (r_{ij} - r_j^0)} \tag{14}$$

where $\gamma_j, (j = 1, 2, \cdots, m)$ is the weight of each decision-making objective obtained by combining the entropy method with the analytic hierarchy process [32].

V. THE BASIC CONCEPT OF BEETLE ANTENNAE SEARCH (BAS)

A. BAS

The Beetle Antennae Search is a bioinspired intelligent optimization algorithm inspired by the foraging principle of beetles, which is based on the smell of food using two antennae. If the left antennae receives a stronger odour than the right antenna, then the next step is to fly to the left and not the right. The beetle can determine the position of the food effectively according to this principle. The smell is regarded as a function, and the optical value of the function can be found by collecting the odour value of two points near the beetle.

The beetle produces a random vector method to determine the direction of food, and the random direction is generated as follows:

$$\vec{d} = \frac{rands(n, 1)}{|rands(n, 1)|} \tag{15}$$

where rand(n,1) represents a random function and n represents the dimension of space. Then, according to the direction

vector, the left and right antennae of the beetle are defined as

$$\begin{aligned} x_l^t &= x^t + d_0 \cdot \vec{d} \\ x_r^t &= x^t - d_0 \cdot \vec{d} \end{aligned} \tag{16}$$

where x_l^t and x_r^t respectively represent the location of the search area on the left and right of the beetle at time t, x^t represents the position of the beetle at time t, and d_0 is the length between the left and right antennae at time t. The odour intensity of the left and right antennae can be defined as $f(x_l^t)$ and $f(x_r^t)$ function, and then we can calculate the position of the beetle at the next moment as follows:

$$x^{t+1} = x^t - \delta^t \cdot \vec{d} \cdot sign(f(x_l^t) - f(x_r^t)) \tag{17}$$

where $f(\cdot)$ is the fitness function, δ^t represents the step size at time t, and sign(·) is a sign function. To search the optimal solution, the step size decrease with the number of iterations increases as follows:

$$\delta^t = \lambda \cdot \delta^{t-1} \tag{18}$$

where λ is the attenuation coefficient of the step length δ. The length d between the right and left antennae, for practical calculation, is variable with step size, and this can be generated by the following formula

$$d_0 = \delta^t / c \tag{19}$$

where c is a constant, generally from 2 to 10.

B. CHAOTIC DISTURBANCE BAS

In the BAS algorithm, because a beetle population is difficult to maintain in the optimization process, the antennae must be an individual search, and it often converges to local optima. To address this shortcoming, a BAS with chaotic disturbance (CDBAS) that combines BAS with a chaotic local search is proposed in this study. First, a beetle that needs chaotic disturbance is found according to the similarity, which is calculated by the similar function (20). Chaotic sequences are generated by the logistic map in this paper (22), which is described as follows:

$$c_i = \begin{cases} 1, & d(i,j) < \dfrac{d_{\max} - d_{\min}}{2} \\ 0, & d(i,j) \geq \dfrac{d_{\max} - d_{\min}}{2} \end{cases} \tag{20}$$

where $d(i,j)$ is the Euclidean distance from individual i to j, i is the beetle with the best fitness, d_{min} is the Euclidean distance of the nearest individual to i, and d_{max} is the Euclidean distance of the beetle farthest from i.

The similarity is described as follows:

$$C = \sum_{i=1}^{N} C_i \tag{21}$$

Logistic map is described as follows:

$$\begin{cases} X_k = \mu X_k^c (1 - X_k^c) & \text{C} > 0.2\text{N} \\ \text{No chaotic disturbance} & \text{if not} \end{cases} \tag{22}$$

TABLE 1. Algorithm 1 CDBAS algorithm.

Algorithm 1 CDBAS algorithm
Input: System parameters, loads and DG, index constraints, and CDBAS algorithm.
Output: the optimal switch combination.
1: Generate 'pbest' beetles to be the initial population number randomly.
2: **tic**
3: **for** i=1: N **do**
4: Evaluate the indexes for these initial beetles.
5: Sort the beetles by using grey target decision-making technique, the best solution 'gbest' is retained by (14).
6: **for** k=1: pbest **do**
7: Each beetle generates the position coordinates of the left and right antennae depending on its decision value. The beetle's antennae length d is reduced according to the given formula: $d^t = r * d^{t-1}$.
8: Chaotic disturbance mechanism is carried out for the beetles by using similarity theory, according to the given formula: $C = \sum_{i=0}^{n} c_i$.
9: Rank the beetles by using grey target decision-making technique, and the best beetle 'gbest' is retained as a basic solution for chaotic disturbance mechanism.
10: **end**
11: **end**
12: Return 'gbest' and corresponding results of each index.

where X_k is the k-dimensional variable of chaotic sequence X, that is, $X_k \in [0, 1]$, $\mu \in (3.569, 4)$, and N is the number of populations.

The chaos initial population is scaled into [0,1], and the chaotic sequence $G = \{X^1, \ldots\ldots, X^S\}$ can be obtained in accordance with iteration (23),

$$newX_k = b_{\min} + (b_{\max} - b_{\min})X_k \tag{23}$$

where b_{max} and b_{min} are the upper and lower boundary values of k-dimensional variable $newX_k$, respectively.

C. MULTIOBJECTIVE CDBAS BASED ON GREY TARGET DECISION-MAKING METHOD

With the aim of adopting the CDBAS algorithm for solving multiobjective optimization problems, a grey target decision-making theory is applied to achieve the power of the beetles, that is for sorting the beetles.

Here, the proposed method randomly generates the initial population of 'pbest' beetles in the specified search range. The corresponding indexes of these initial beetles are calculated and then sorted by using the grey target decision-making technique. Furthermore, each beetle generates the left and right antennae spatial position coordinates depends upon its decision value. The chaotic disturbance mechanism is carried out for better beetles depending on the best beetle and each beetle generates a new position according to the left and right antennae spatial position coordinates. The population is again ranked, and this computation continues until the specified target condition is reached. Moreover, Table 1 and Fig. 3 show the procedure process and the flowchart of the CDBAS method.

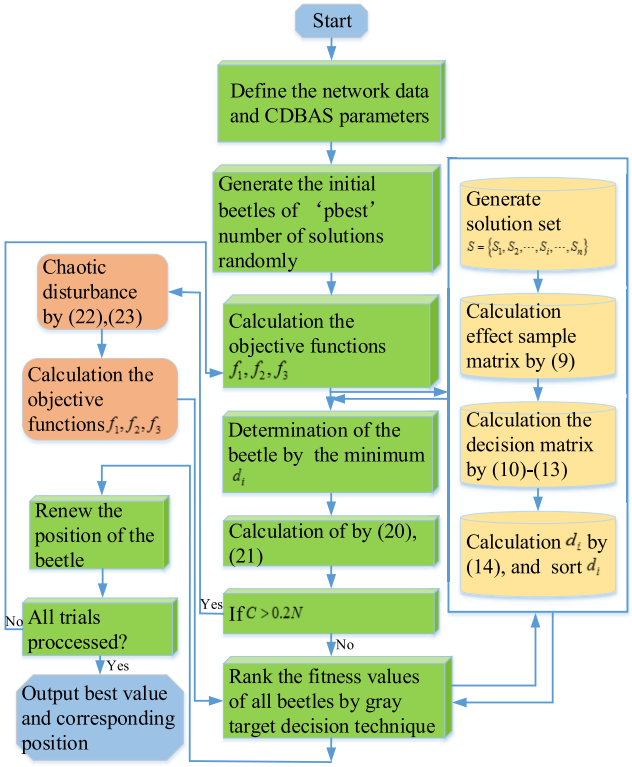

FIGURE 3. Flowchart of the proposed CDBAS algorithm.

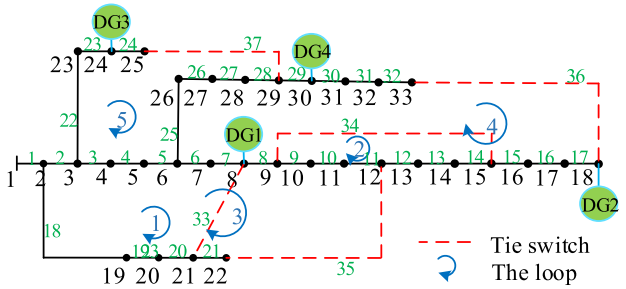

FIGURE 4. Simplified diagram of the IEEE 33-bus distribution network.

VI. SIMPLIFICATION AND ENCODING OF TOPOLOGY BASED ON BASIC LOOP

A. OPTIMAL NETWORK RECONFIGURATION

In general, the optimal network reconfiguration is achieved by changing the status of the switches including normally closed switches and normally open switches, while satisfying the constraint in any distributed system. Only tie-line switches are allowed to be open, and the other switches are closed to generate a solution vector to reduce the computational speed of the system. With the aim of generating fewer infeasible solutions, all switches are initially closed, and then only one switch is selected to be open for each loop under the condition of satisfying the constraints, which are the radiation and connectivity of the network structure. In addition, the number of open switches (*i.e.,* tie switches) is defined as the size of the problem decision variable.

TABLE 2. Loop vectors of the 33 bus radial distribution system.

Loop	All switches
Loop1	8,7,6,5,4,3,2,18,19,20,21,33
Loop2	9,10,11,12,13,14,34
Loop3	11,10,9, 8,7,6,5,4,3,2,18,19,20,21,35
Loop4	32,31,30,29,28,27,26,25,6,7,8,9,10,11,12,12,14,15,16,17,26
Loop5	24,23,22,3,4,5,25,26,27,28,37

For example, the modified IEEE 33-bus radial network which is represented in Fig. 4 below is considered to evaluate the performance of the proposed methodology. In this network, the number of normally open switches is 5, and the CDBAS algorithm generates a 5-dimensional vector as the size of the problem decision variable based on the condition of satisfying the constraints. However, the indexes are calculated according to the generated feasible solution which is to maintain the radial and connected network structure, and the generated unfeasible solution can be replaced by generating a new solution immediately. To detect the radial network structure, an incidence matrix is generated according to the distribution network topology in Fig. 4.

We adopt the encoding method of particles based on the loop topology by which only one switch can be selected in each loop. Table 2 shows loop vectors formed according to the distribution network topology in Fig. 4. The binary numbers 0 and 1 are used to encode the open and closed states of the contact switch. In (24), (1 or 0) means take '1' or '0', and D_{ij} represents the opening and closing state of the j section switch in loop 'i'. When (1or0) is taken to 1, the contact switch of loop 'i' is closed, and D_{ij} indicates that the segment switch 'j' of loop '1' is disconnected. When (1 or 0) is taken to 0, the segment switch 'j' in D_{ij} takes a random number, in other words, the contact switch in loop 'i' is disconnected, and the segment switch is closed.

$$\{(1\ or\ 0)|(D_{1j})|\cdots(1\ or\ 0)|(D_{ij})|\cdots|(1\ or\ 0)|(D_{Nj})\} \quad (24)$$

B. CDBAS METHODOLOGY FOR OPTIMAL MULTIOBJECTIVE RECONFIGURATION

With the CDBAS methodology used for solving the multiobjective network reconfiguration problem for the distribution system, each beetle is defined as a solution vector consisting of open switches. The randomly generated dimension of the initial population is the number of switches to be opened in the system, and it moves to the optimal reconfiguration solution step by step through the iteration update of the orientation position. The position of the beetle is used to simulate the switching state of each one-dimensional switch. The fitness value in the CDBAS approach for optimal network reconfiguration is the distance d_i of the grey target decision-making design for the three indexes in the system including active power loss, load balancing and maximum node voltage deviation, as described in Section III. The solution corresponding to the minimum value of distance d_i is obtained in accordance with the ranking of the distance d_i. Next, the population is

ranked by using grey target decision-making theory, and the population is updated by using the CDBAS method. Furthermore, the generated feasible solution obtained for optimal network reconfiguration by the proposed method must satisfy the radial constraint and be feasible to provide services for all the loads with the level values of voltage and current. If the generated solution violates one of the constraints set in this study, the solution is discarded.

VII. EXPERIMENTAL DESIGN AND RESULTS ANALYSIS

A. EXPERIMENTAL DESIGN

1) BENCHMARK FUNCTIONS

To verify the performance of the proposed CDBAS algorithm, 8 benchmark functions are tested in the simulation. Table 3 shows the expressions, dimensions, search ranges and theoretical optimal values of 8 benchmark functions. The functions g1-g3 are typical unimodal functions, which are mainly used to test the accuracy, convergence rate and global search ability of the algorithm. The g4-g8 functions are continuous multimodal functions and have an infinite number of local minimum points centered on the global minimum and the radial ring region. Therefore, these functions are often used to test the global optimization ability, the convergence rate and the local optimal avoidance ability of the algorithm.

Here, to set the parameters of the CDBAS and BAS algorithms, the initial population size of the beetles is 100, the maximum number of iterations is 200, the descending coefficient of longicorn step size is $\lambda = 0.95$, the degradation factor of step size to beetle antennae is $c = 5$, and the initial maximum step size is $\delta = 1$.

The two algorithms run independently 30 times, and the search dimension of each function is 5, 10 and 30. Then, the performance of the algorithm is compared and analysed by comparing the accuracy of the results and the evolution curve.

2) ALGORITHM ACCURACY COMPARISON

The precision and robustness of the algorithm are evaluated by the optimal value, the worst value, the average value and square difference tested benchmark functions with 5, 10 and 30 dimensions, which are shown in Table 4, Table 5 and Table 6, respectively.

Taking the functions g1-g3 in Table 4, Table 5 and Table 6 as an example, the precision of the CDBAS algorithm is higher than that of the BAS algorithm and the robustness is better. From the comparison results for the functions g4-g8, the CDBAS also enhanced the global search ability; it was very easy to avoid the local optimal pole since the temporal perturbation decreased continuously with the increase of the supernumerary number.

VIII. TEST AND ANALYSIS OF CDBAS ALGORITHM FOR DISTRIBUTION NETWORK RECONSTRUCTION

To validate the presented method and compare it with other methods, the optimal network reconfiguration is solved for the following cases:

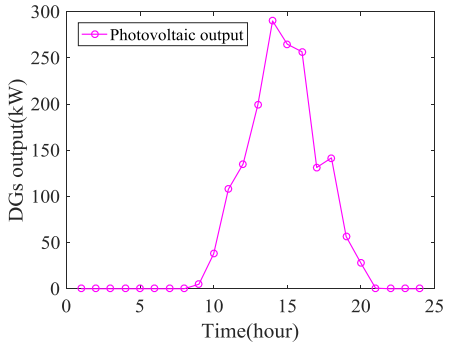

(a) The output distribution of Photovoltaic

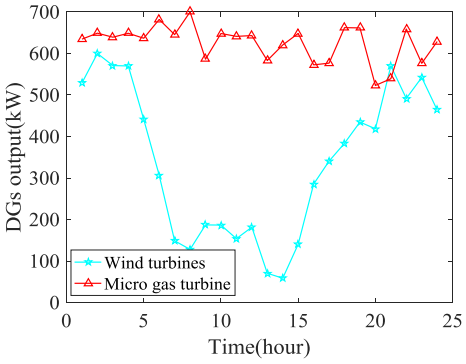

(b) The output distribution of wind turbine and micro gas turbine

FIGURE 5. The output distribution of DG in 24 hours.

Case-1. Minimization of active power loss with reconfiguration one time over 24 hours

Case-2. Minimization of the load balancing index with reconfiguration one time over 24 hours

Case-3. Minimization of maximum node voltage deviation with reconfiguration one time over 24 hours

Case-4. Simultaneous minimization of active power loss, load balancing index and maximum node voltage deviation with reconfiguration one time over 24 hours

Case-5. Simultaneous minimization of active power loss, load balancing index and maximum node voltage deviation with reconfiguration five times over 24 hours

Case-6. Simultaneous minimization of active power loss, load balancing index and maximum node voltage deviation with reconfiguration twenty-four times over 24 hours

A. 33-BUS TEST SYSTEM

The performance and effectiveness of the presented methodology is verified on the modified IEEE 33-Bus system and compared with other methods. Fig. 4 shows single diagram of this network with 4 DG networks. The specific parameters and the locations of DG access are shown in Table 7. Table 8 and Table 9 show the proportion load and distribution in hours for three types of load in each bus and for that considered in the study case on the modified IEEE 33 bus network [33]. Fig. 5 shows the output distribution of DGs in 24 hours.

TABLE 3. Benchmark functions.

Name	Function	Dim	Range	gmin
Sphere	$g_1(x)=\sum_{i=1}^{d}x_i^2$	5	[-10, 10]	0
Rosenbrock	$g_2(x)=\sum_{i=1}^{d-1}\left[100\left(x_{i+1}-x_i^2\right)^2+\left(x_i-1\right)^2\right]$	5	[-10, 10]	0
Step	$g_3(x)=\sum_{i=1}^{D}\left[x_i+0.5\right]^2$	5	[-10, 10]	0
Ackley	$g_4(x)=-20\exp[-0.2\sqrt{\frac{1}{d}\sum_{i=1}^{d}x_i^2}]-\exp\left[\frac{1}{d}\sum_{i=1}^{d}\cos\left(2\pi x_i\right)\right]$	5	[-10, 10]	0
Rastrigin	$g_5(x)=10d+\sum_{i=1}^{d}\left[x_i^2-10\cos\left(2\pi x_i\right)\right]$	5	[-10, 10]	0
Levy	$g_6(x)=\sin^2\left(\pi z_i\right)+\sum_{i=1}^{n-1}\left(z_i-1\right)^2\left[1+10\sin^2\left(\pi z_i+1\right)\right]+\left(z_i-1\right)^2\left[1+\sin^2\left(2\pi z_i\right)\right]$	5	[-10,10]	0
Dixon-Price	$g_7(x)=\left(x_1-1\right)^2+\sum_{i=2}^{d}i\left(2x_i^2-x_{i-1}\right)^2$	5	[-10,10]	0
Michalewicz	$g_8(x)=-\sum_{i=1}^{d}\sin\left(x_i\right)\sin^{2m}\left(\frac{ix_i^2}{\pi}\right)$	5	[0, π]	-4.68766

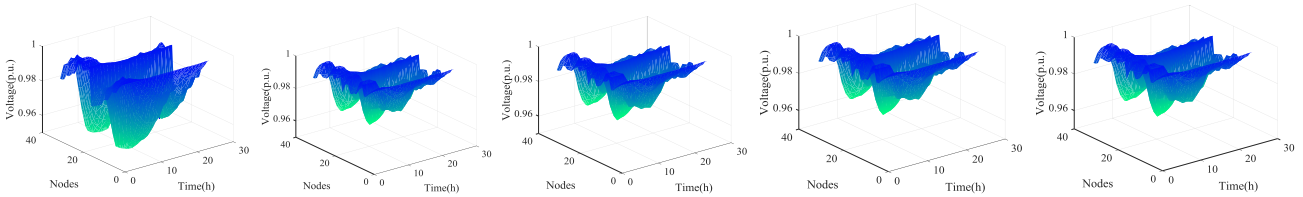

(a) Original system (b) CDBAS algorithm (c) PSO algorithm (d) GA algorithm (e) BAS algorithm

FIGURE 6. Voltage profile of the 33 bus networks with DG for 24 hours.

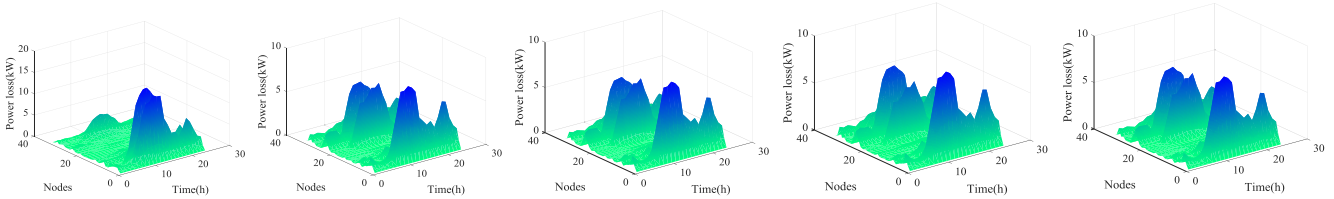

(a) Original system (b) CDBAS algorithm (c) PSO algorithm (d) GA algorithm (e) BAS algorithm

FIGURE 7. Power loss profile of the 33 bus networks with DG over 24 hours.

1) VALIDATION OF CDBAS ALGORITHM

The simulation results of IEEE 33-node systems with DG for Cases 1, 2, 3 and 4 are given in Table 10. From the results shown for Cases 1, 2 and 3 in Table 10, the optimal solution obtained by the proposed algorithm is better than the results obtained in reference [16] and [34]. We can see that the indexes conflict with each other to minimize each index simultaneously to achieve the optimal solution. A comprehensive solution with three objectives considering the numbers of the switching operations index for the optimal operation of the distribution system is studied and obtained in Case 4. In addition, the total running time for optimal reconfiguration proposed algorithm in Case 4 is 90.99 s which has been reduced 132.73 s and 95.23 s in comparison with algorithm used in [16] and [34], respectively.

2) VERIFICATION OF ALGORITHM SUPERIORITY

Fig. 6, Fig. 7, and Fig. 8 show the node voltage distribution (standard unitary value), power loss and load balance of the network before and after reconfiguration with DG based on

TABLE 4. Performance comparison of eight functions when the search dimension is 5 - D.

Function	Algorithm	Min	Max	Mean	Std
g1	BAS	2.87E-09	21.0864	0.8590	3.1465
	CDBAD	2.74E-10	28.1357	0.2108	2.0629
g2	BAS	3.631832	23286.5	491.01	2182.58
	CDBAD	0.002134	25526.6	132.14	1800.57
g3	BAS	0.199188	60.7465	3.8084	10.2879
	CDBAD	1.46E-10	8.00586	0.0838	0.6327
g4	BAS	4.662396	6.23432	4.8207	0.3519
	CDBAD	2.01E-05	8.37930	0.2187	0.7369
g5	BAS	19.89912	83.9379	23.039	7.5595
	CDBAD	1.989918	44.2729	2.8613	3.4673
g6	BAS	2.661713	11.1671	2.8905	0.7524
	CDBAD	1.16E-10	5.90420	0.0405	0.4287
g7	BAS	0.791491	1061.37	21.2476	108.17
	CDBAD	2.52E-06	642.682	3.5580	45.3830
g8	BAS	-3.95807	-1.9696	-3.6619	0.3614
	CDBAD	-4.6459	-1.7953	-4.3530	0.5022

TABLE 5. Performance comparison of eight functions when the search dimension is 10 - D.

Function	Algorithm	Min	Max	Mean	Std
g1	BAS	44.51857	131.385	51.8854	16.0775
	CDBAS	2.61E-09	131.9895	0.9192	9.4616
g2	BAS	27054.55	282696.1	44903.5	42854.4
	CDBAS	1.543409	311573.1	1589.84	21974.7
g3	BAS	36.76735	131.2202	44.3479	16.5185
	CDBAS	1.51E-09	170.4503	1.2885	12.2049
g4	BAS	9.473361	11.57903	9.7775	0.5471
	CDBAS	0.005384	10.72807	0.5785	1.2065
g5	BAS	132.4149	260.2307	146.61	24.9110
	CDBAS	4.976304	234.7365	12.4445	20.5692
g6	BAS	6.818	38.99361	7.9337	3.7729
	CDBAS	0.049731	24.1843	0.3081	1.7691
g7	BAS	7251.713	56030.9	11444.8	9946.48
	CDBAS	0.666823	44601.79	243.29	3149.69
g8	BAS	-6.89082	-3.81419	-5.9854	1.0940
	CDBAS	-8.45474	-3.1251	-7.3901	1.4311

TABLE 6. Performance comparison of eight functions when the search dimension is 30 - D.

Function	Algorithm	Min	Max	Mean	Std
g1	BAS	504.1234	614.7341	516.126	23.7369
	CDBAS	4.114349	625.2035	10.4461	44.5750
g2	BAS	1279450	2142033	1362497	167864
	CDBAS	392.8495	1458568	8584.62	102859
g3	BAS	493.6879	645.1843	508.02	29.8937
	CDBAS	8.634809	578.4035	16.5156	41.9549
g4	BAS	11.86322	12.99106	12.0645	0.3007
	CDBAS	2.983314	13.42507	3.3847	0.9806
g5	BAS	804.7249	1011.373	829.59	39.9880
	CDBAS	55.80578	971.2369	94.7385	82.4684
g6	BAS	85.53	172.75	95.2692	19.0005
	CDBAS	2.837398	164.4318	4.3520	11.5809
g7	BAS	0.791491	1061.367	21.2476	108.17
	CDBAS	2.52E-06	642.6815	3.5580	45.3830
g8	BAS	-12.3822	-6.16081	-10.876	1.5648
	CDBAS	-16.086	-6.64302	-13.901	2.3632

Case 4 using CDBAS, Particle Swarm Optimization (PSO) in [16], Genetic Algorithm (GA) in [34] and BAS for the distribution network. The results show that the three indexes of the proposed methodology are better than those of the other three methods for distribution network reconfiguration considering variations in load and DG over 24 hours.

TABLE 7. The specific parameters and the locations of DG access to IEEE 33-Bus system.

	Location	Type	Capacity	Power factor
DG1	8	Wind turbine	600kW	0.95
DG2	18	Photovoltaic panels	300kW	0.95
DG3	24	Micro gas turbine	700kW	0.95
DG4	30	Wind turbine	600kW	0.95

TABLE 8. The proportion of three types of load in each bus.

Nodes	Residential/Industrial/ Commercial load			Nodes	Residential/Industrial/ Commercial load		
2	0.5	0.3	0.2	18	0.5	0.1	0.4
3	0.3	0.2	0.5	19	0.2	0.3	0.5
4	0.2	0.3	0.5	20	0.3	0	0.7
5	0.1	0.3	0.6	21	0.3	0.2	0.5
6	0.4	0.2	0.4	22	0	0.7	0.3
7	0	0.4	0.6	23	0.4	0.1	0.5
8	0.3	0.4	0.3	24	0.5	0.1	0.4
9	0.6	0	0.4	25	0.4	0	0.6
10	0	0.7	0.3	26	0.3	0	0.7
11	0.2	0.2	0.6	27	0	0.9	0.1
12	0.5	0	0.5	28	0.3	0.1	0.6
13	0.4	0	0.6	29	0.1	0.5	0.4
14	0.4	0.2	0.4	30	0.2	0.1	0.7
15	0.1	0.4	0.5	31	0.4	0.2	0.4
16	0.7	0.1	0.2	32	0.1	0.7	0.2
17	0.3	0.4	0.3	33	0.7	0	0.3

TABLE 9. The load distribution in hours of three types of load.

Hours	Residential/Industrial/ Commercial load			Hours	Residential/Industrial/ Commercial load		
1	0.1	0.3	0.1	13	0.7	0.5	0.6
2	0.1	0.3	0.1	14	0.6	0.6	0.7
3	0.1	0.4	0	15	0.5	0.8	0.8
4	0.1	0.2	0	16	0.6	0.8	1
5	0.4	0.2	0	17	0.7	0.7	1
6	0.3	0.3	0	18	0.8	0.7	0.8
7	0.4	0.3	0.1	19	0.9	0.8	0.6
8	0.4	0.4	0.2	20	1	0.9	0.7
9	0.3	0.8	0.7	21	1	1	0.6
10	0.3	1	0.8	22	0.6	0.8	0.2
11	0.5	0.9	0.8	23	0.5	0.5	0.1
12	0.6	0.9	0.7	24	0.2	0.4	0.1

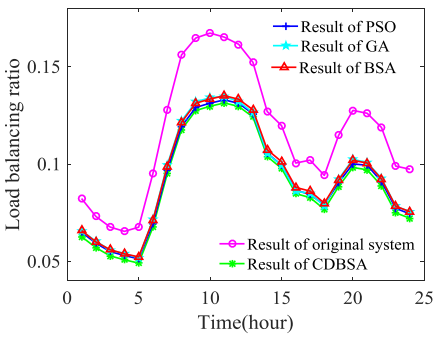

FIGURE 8. Load balance profile of 33 bus networks with DG over 24 hours.

TABLE 10. Simulative results of the IEEE 33-bus system with DG.

Cases	Methods	Open switches	Active power loss (kWh)	Load balancing index (p.u)	Maximum node voltage deviation (p.u)	Running time (s)	No. of switching operations
	Original system	33 34 35 36 37	857.54	2.7733	0.8660	–	–
Case-1	CDBAS	7 14 11 17 28	574.30	2.2571	0.4995	94.33	10
	PSO in [16]	7 14 10 32 28	574.69	2.2745	0.5282	232.72	10
	GA in [34]	7 13 10 16 28	588.01	2.2753	0.5492	199.72	10
	BAS	7 13 9 16 28	588.52	2.2634	0.5449	99.53	10
Case-2	CDBAS	7 13 10 16 27	596.41	2.2246	0.5635	97.33	10
	PSO in [16]	7 13 10 17 27	590.45	2.2264	0.5226	235.72	10
	GA in [34]	7 13 10 17 27	590.45	2.2264	0.5226	187.94	10
	BAS	6 14 11 15 28	616.49	2.3195	0.5925	94.50	10
Case-3	CDBAS	7 14 11 17 28	574.30	2.2571	0.4995	93.91	10
	PSO in [16]	7 12 9 17 28	589.22	2.2779	0.51406	221.72	10
	GA in [34]	7 13 9 16 28	588.52	2.2634	0.5449	179.02	10
	BAS	7 12 9 17 28	589.22	2.2779	0.51406	91.11	10
Case-4	CDBAS	7 14 11 17 28	574.30	2.2551	0.4995	90.99	10
	PSO in [16]	7 14 10 17 28	574.77	2.2572	0.5004	223.72	10
	GA in [34]	7 14 10 32 27	580.86	2.2600	0.5066	186.22	10
	BAS	7 14 11 17 27	581.08	2.2437	0.5037	93.65	10

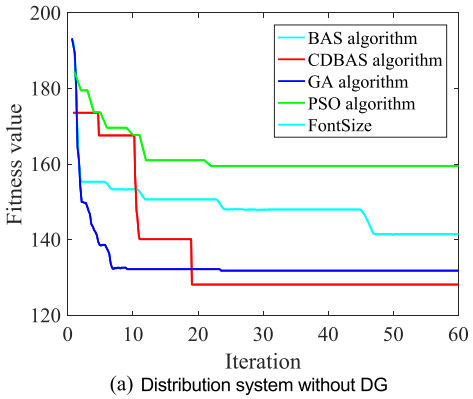

(a) Distribution system without DG

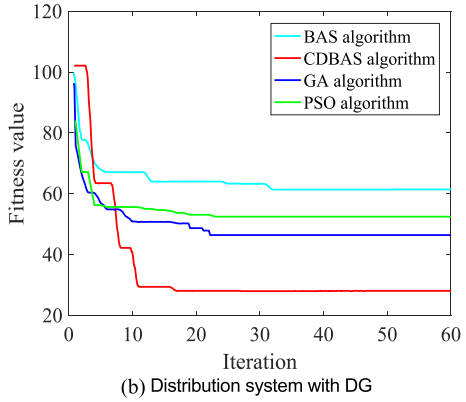

(b) Distribution system with DG

FIGURE 9. Global convergence curves of the proposed algorithm and algorithms in reference [16] and [34].

The voltage profiles of the 33 bus networks before and after reconfiguration during for 24 hours are illustrated in Fig. 6. It is clear that the minimum voltage amplitude of each algorithm is 0.9450 p.u. at 11 a.m, 0.9650 p.u. at 9 p.m, 0.9635p.u. at 9 p.m, 0.9620 p.u. at 9 a.m, and 0.9631 p.u. at 9 a.m.

Fig. 7 shows the power loss profile of the 33 bus network before and after reconfiguration with DG for 24 hours.

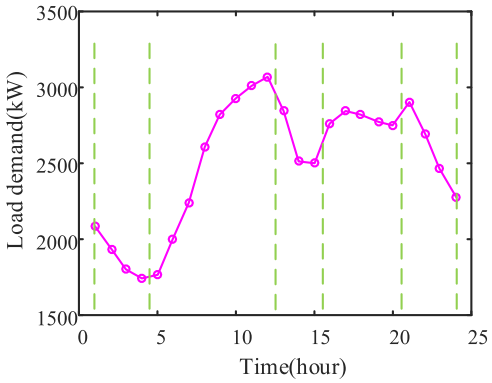

FIGURE 10. Total load demand curve over 24 hours.

It is clear that the maximum total power loss of each algorithm for the distribution network over 24 hours is 857.54 kWh, 574.77 kWh, 574.77 kWh, 580.86 kWh, and 581.08 at 12 a.m.

From the results of Fig. 6 voltage and Fig. 7 active power loss, we can see that the voltage and active power loss results of CDBAS algorithm are slightly better to compare the PSO algorithm [16], the GA algorithm [34] and the BAS algorithm. In other words, the CDBAS algorithm is better in global optimization ability.

Fig. 8 shows the load balance before and after reconfiguration for 24 hours. The results show that the total load balance value for each algorithm over 24 hours is 2.7733, 2.2551, 2.2572, 2.2600 and 2.2437

3) EFFICIENCY VERIFICATION OF ALGORITHMS

From the results shown for the population evolution of the four algorithms in Fig. 9, the number of iterations and global optimization capability of the CDBAS algorithm are better than those of the other three algorithms. The minimum number of iterations of the CDBAS algorithm is

TABLE 11. Real-time results of Cases 5 and 6 of the 33-bus system over 24 hours.

Hour	Open switches		Active power loss (kW)			Load balancing index (p.u)			Maximum node voltage deviation index (p.u)			Numbers of switching operations	
	Case-5	Case-6	Original system /Case5/ Case-6			Original system/Case-5/ Case-6			Original system/Case-5/ Case-6			Case-5/ Case-6	
1		6 14 11 16 27	12.75	9.53	9.91	0.0823	0.0659	0.0648	0.0225	0.0125	0.0143		
2	6 14 10	6 14 11 17 37	9.56	7.52	7.74	0.0731	0.0624	0.0562	0.0161	0.0092	0.0091		
3	32 37	6 13 10 16 26	8.42	6.54	6.54	0.0676	0.0521	0.0521	0.0147	0.0074	0.0074		
4		6 14 11 17 37	7.77	5.99	6.19	0.0654	0.0543	0.0494	0.0136	0.0069	0.0064		
5		6 13 10 17 37	8.47	5.97	7.50	0.0676	0.0542	0.0581	0.0199	0.0099	0.0126		
6		7 14 11 17 28	18.48	11.41	12.05	0.0952	0.0716	0.0747	0.0305	0.0153	0.0194		
7		33 14 9 36 28	39.13	23.68	24.19	0.1280	0.1001	0.1008	0.0427	0.0232	0.0285		
8	7 14 9 32	7 14 9 36 28	61.43	36.65	36.85	0.1561	0.1222	0.1233	0.0518	0.0285	0.0333		
9	28	7 14 10 32 28	71.64	43.35	43.17	0.1648	0.1320	0.1327	0.0532	0.0313	0.0307		
10		7 14 9 32 28	75.61	44.81	44.81	0.1673	0.1347	0.1347	0.0539	0.0317	0.0317		
11		7 14 10 32 28	77.11	47.51	47.54	0.1652	0.1343	0.1351	0.0550	0.0337	0.0337		
12		7 14 10 32 28	73.22	45.82	45.94	0.1615	0.1320	0.1327	0.0537	0.0332	0.0332		
13		7 14 9 17 28	67.48	44.47	44.86	0.1523	0.1283	0.1338	0.0518	0.0310	0.0344		
14	7 14 9 32 28	7 14 9 31 28	46.17	28.36	28.74	0.1270	0.1057	0.1060	0.0441	0.0247	0.0228	28	88
15		7 14 9 31 28	39.70	24.81	24.96	0.1198	0.1024	0.1023	0.0407	0.0256	0.0227		
16		7 14 11 31 28	25.99	18.35	19.65	0.1005	0.0887	0.0864	0.0314	0.0208	0.0218		
17		7 14 11 32 28	25.70	19.00	19.14	0.1020	0.0851	0.0852	0.0293	0.0197	0.0197		
18	33 10 7 32 28	7 13 10 32 28	20.73	15.85	15.92	0.0942	0.0780	0.0788	0.0254	0.0164	0.0164		
19		7 14 11 32 28	29.40	20.82	21.22	0.1147	0.0940	0.0950	0.0349	0.0203	0.0235		
20		7 14 10 32 28	37.09	26.00	26.75	0.1276	0.1037	0.1062	0.0407	0.0235	0.0287		
21		7 14 11 32 28	33.68	24.36	24.42	0.1261	0.1025	0.1008	0.0405	0.0238	0.0222		
22	7 14 11	7 14 11 36 27	29.59	19.81	19.75	0.1188	0.0930	0.0937	0.0384	0.0192	0.0192		
23	36 28	7 14 11 36 27	19.43	14.04	14.07	0.0989	0.0786	0.0793	0.0316	0.0149	0.0147		
24		33 14 7 36 27	18.99	12.94	12.95	0.0974	0.0763	0.0766	0.0298	0.0153	0.0142		
			857.54	557.59	564.87	2.7733	2.2520	2.2587	0.8660	0.4981	0.5207		
Total energy loss (kWh), load balancing index, maximum node voltage deviation, and numbers of switching operations during 24 hours													

TABLE 12. The specific parameters and the locations of DG access to IEEE 69-Bus system.

	Location	Type	Capacity	Power factor
DG1	26	Micro gas turbine	100kW	0.95
DG2	39	Photovoltaic panels	150kW	0.95
DG3	54	Wind turbine	200kW	0.95
DG4	68	Wind turbine	200kW	0.95

19 times and 17 times for the IEEE 33-bus distribution system without DG in Fig. 9 (a) and with DG in Fig. 9 (b), respectively.

4) OPTIMAL RECONFIGURATION IN TIME SEGMENTS

The number of network reconfigurations is set to five for one day over 24 hours considering the limit of switching action based on the load demand curve. In Fig. 10 shows the total demand profile over 24 hours. The five network reconfiguration periods in a day are 1-4, 5-12, 13-15, 16-20, and 21-24. The reconfiguration results of Cases 5 and 6 are given in Table 11 to compare the two cases for different switching times during 24 hours. It is clear that the total power loss of 557.59 kWh, the total load balancing index of 2.2520 and the total maximum node voltage deviation of 0.4981 in Case 5 are both better than total power loss of 564.87 kWh, the total load balancing index of 2.2587 and the total maximum node voltage deviation of 0.5207 in Case 6 over 24 hours.

B. 69-BUS TEST SYSTEM

In this section, multi-objective reconfiguration of the distribution network is done, with the objectives of active power loss, load balancing index and Maximum node voltage deviation. The CDBAS algorithm is used for optimization and reconfiguration are implemented on the modified IEEE 69-bus system. In 69 bus standard system there are five loops so it should have five tie switches to remain network radial in [35]. The specific parameters and the locations of DG access are shown in Table 12.

The proportion load and distribution in hours for three types of load in each bus are presented in [35] and for that considered in the study case on the modified IEEE 69 bus network. In Fig. 10 shows the total demand profile over 24 hours. The optimization results of the improved algorithm for Case 4 are given and compared with results of [16] in Table 13.

From Table 13 for Case 4, the best solution given by proposed method is better than the results obtained in reference [16]. The total active power loss is reduced by 39.62%, minimum node voltage is improved from 0.9278 to 0.9536 in Fig. 11 and the number of switching operations is 14.

The reconfiguration results of Cases 5 and 6 are given in Table 14 to compare the two cases for different switching times during 24 hours. It is clear that the total power loss of 781.77 kWh, load balancing of 2.6710 and the total maximum node voltage deviation of 0.7580 in Case 5 are both slightly

TABLE 13. Results of Cases 4 for the IEEE 69-bus system with DG.

Cases	Methods	Open switches	Active power loss (kWh)	Load balancing index (p.u)	Maximum node voltage deviation (p.u)	Running time (s)	No. of switching operations
Case-4	Original system	69,70,71,72,73	1296.1	2.6888	1.1049	–	0
	CDBAS	69 70 14 50 44	782.59	2.6621	0.7570	102.73	6
	PSO in [16]	69 70 12 50 47	782.93	2.6787	0.75802	255.06	6
	BAS	10 70 14 50 46	815.65	2.8508	0.7589	101.95	8

TABLE 14. Real-time results of Cases 5 and 6 of the 69-bus system over 24 hours.

Hour	Open switches		Active power loss (kW)			Load balancing index (p.u)			Maximum node voltage deviation index (p.u)			Numbers of switching operations	
	Case-5	Case-6	Original system /Case5/ Case-6			Original system/Case-5/ Case-6			Original system/Case-5/ Case-6			Case-5/ Case-6	
1	69 70 12 50 45	69 70 14 50 47	32.71	19.06	19.53	0.0877	0.0833	0.0857	0.0371	0.0251	0.0251		
2		10 70 13 25 46	23.83	15.63	15.73	0.0805	0.0741	0.0745	0.0324	0.0232	0.0238		
3		10 70 13 24 44	19.23	13.55	13.89	0.0750	0.0685	0.0683	0.0302	0.0222	0.0223		
4		69 70 14 50 47	16.93	12.26	12.39	0.0723	0.0614	0.0665	0.0288	0.0205	0.0208		
5		69 70 12 50 45	23.09	14.89	14.94	0.0950	0.0704	0.0699	0.0333	0.0228	0.0228		
6		69 70 13 50 44	39.15	21.36	21.37	0.1872	0.0889	0.0886	0.0416	0.0269	0.0269		
7	69 70 14 50 46	69 70 14 50 46	69.34	34.20	34.20	0.1043	0.1101	0.1101	0.0545	0.0346	0.0346		
8		69 70 14 50 45	84.31	49.80	49.80	0.1235	0.1289	0.1289	0.0557	0.0424	0.0424		
9		69 70 14 50 46	92.40	54.34	54.34	0.1306	0.1369	0.1369	0.0571	0.0442	0.0442		
10		69 70 14 50 45	106.02	59.63	59.63	0.1360	0.1423	0.1423	0.0610	0.0464	0.0464		
11		69 70 14 50 46	106.97	58.89	58.89	0.1391	0.1488	0.1488	0.0612	0.0450	0.0450		
12		69 70 14 50 45	111.54	60.79	60.79	0.1407	0.1501	0.1501	0.0622	0.0458	0.0458		
13	69 70 14 50 46	69 70 14 50 46	88.87	49.96	49.96	0.1323	0.1460	0.1460	0.0566	0.0397	0.0397		
14		69 70 14 50 44	61.26	37.61	37.61	0.1148	0.1267	0.1267	0.0485	0.0341	0.0341	14	80
15		69 70 14 50 46	53.20	34.18	34.18	0.1111	0.1236	0.1236	0.0452	0.0318	0.0318		
16		69 13 12 50 44	41.24	29.59	29.48	0.1047	0.1158	0.1151	0.0497	0.0293	0.0293		
17	69 70 13 50 46	69 70 12 50 45	35.65	24.29	24.29	0.1005	0.1090	0.1090	0.0424	0.0261	0.0261		
18		69 13 12 50 45	30.43	22.24	22.20	0.0973	0.1035	0.1030	0.0400	0.0251	0.0251		
19		69 13 12 50 45	40.02	27.01	26.96	0.1086	0.1157	0.1151	0.0431	0.0274	0.0274		
20		69 70 13 50 47	45.63	29.77	29.77	0.1138	0.1224	0.1224	0.0449	0.0287	0.0287		
21	69 70 12 50 46	69 70 12 50 45	52.68	33.03	33.17	0.1204	0.1239	0.1245	0.0468	0.0312	0.0312		
22		69 70 12 50 45	44.72	28.75	28.90	0.1114	0.1166	0.1173	0.0450	0.0288	0.0288		
23		69 70 12 50 45	39.66	26.20	26.32	0.1041	0.1047	0.1053	0.0436	0.0286	0.0286		
24		69 13 12 50 44	37.26	24.75	24.82	0.0978	0.0994	0.0998	0.0438	0.0282	0.0282		
			1296.1	781.77	783.16	2.6888	2.6710	2.6784	1.1049	0.7580	0.7591		
Total energy loss (kWh), load balancing index, maximum node voltage deviation, and numbers of switching operations during 24 hours													

TABLE 15. The specific parameters and the locations of DG access to IEEE 118-Bus system.

	Location	Type	Capacity	Power factor
DG1	25	Photovoltaic panels	1.5MW	0.95
DG2	35	Photovoltaic panels	1.5MW	0.95
DG3	46	Wind turbine	1.5MW	0.95
DG4	54	Wind turbine	1.5MW	0.95
DG5	72	Wind turbine	3MW	0.95
DG6	85	Wind turbine	1.5MW	0.95
DG7	99	Wind turbine	1.5MW	0.95
DG8	111	Wind turbine	2.25MW	0.95

better than total power loss of 783.16 kWh load balancing of 2.6784 and the total maximum node voltage deviation of 0.7591 in Case 6 over 24 hours.

C. 118-BUS TEST SYSTEM

The IEEE 118-bus system consists of 118 buses, 11 kV, and radial distribution system [36]. In 118 bus standard system there are fifteen loops so it should have 117 sectional switches and 15 tie switches to remain network radial. The CDBAS algorithm is used for optimization and reconfiguration are implemented on the modified IEEE 118-bus system. In this section, the reconfiguration results of Cases 4, 5 and 6 by the CDBAS algorithm are presented and compared with the results of [16]. The specific parameters and the locations of DG access are shown in Table 15 [37]. In Fig. 12 shows the total demand profile over 24 hours.

From Table 16 for Case 4, the best solution given by proposed method is better than the results obtained in reference [16]. The total active power loss is reduced by 10.99%, minimum node voltage is improved from 0.8847 to 0.9335 in Fig. 13 and the number of switching operations is 104.

The reconfiguration results of Cases 5 and 6 are given in Table 17 and 18 to compare the two cases for different switching times during 24 hours. It is clear that the total power loss of 6454.10 kWh, the load balancing of 1.8900 and the

TABLE 16. Results of Cases 4 for the IEEE 118-bus system with DG.

Cases	Methods	Open switches	Active power loss (kWh)	Load balancing index (p.u)	Maximum node voltage deviation (p.u)	Running time (s)	No. of switching operations
Case-4	Original system	119 120 121 122 123 124 125 126 127 128 129 130 131 132 133	8947.80	2.2894	1.8041	–	–
	CDBAS	37 11 23 50 47 59 8 125 71 127 76 80 130 117 33	7964.37	1.9271	0.9242	339.41	22
	PSO in [16]	44 24 20 52 48 58 4 95 126 70 96 105 85 109 10	8150.65	2.0508	1.3589	592.71	28
	BAS	39 19 10 47 48 56 8 55 90 85 98 81 85 117 9	8784.62	2.4977	1.2814	371..88	28

TABLE 17. Real-time results of Cases 5 of the 118-bus system over 24 hours.

Hour	Open switches	Active power loss (kW)		Load balancing index (p.u)		Maximum node voltage deviation index (p.u)		Numbers of switching operations
	Case-5	Original system /Case5		Original system /Case-5		Original system /Case-5		Case-5
1		349.19	303.48	0.0874	0.0856	0.0807	0.0374	
2	38 25 22 50 47 59 124 95	294.25	249.51	0.0805	0.0779	0.0742	0.0324	
3	65 73 96 80 85 115 31	241.95	192.15	0.0736	0.0723	0.0684	0.0261	
4		197.08	137.92	0.0714	0.0694	0.0614	0.0182	
5		234.33	119.85	0.0794	0.0703	0.0603	0.0190	
6		270.47	135.94	0.0840	0.0761	0.0707	0.0123	
7		314.95	172.64	0.0902	0.0843	0.0777	0.0174	
8	40 14 19 49 47 58 5 55	383.35	260.08	0.0990	0.0991	0.0848	0.0241	
9	67 74 75 82 101 117 34	403.74	309.82	0.1034	0.1057	0.0815	0.0276	
10		431.84	425.58	0.1061	0.1063	0.0772	0.0464	
11		405.04	407.18	0.1059	0.1039	0.0668	0.0455	
12		409.97	442.22	0.1072	0.1066	0.0607	0.0507	
13	40 25 20 49 122 58 38 95	301.42	264.54	0.0966	0.0995	0.0468	0.0323	104
14	88 70 75 106 130 131 32	226.45	184.13	0.0856	0.0860	0.0364	0.0207	
15		239.11	184.70	0.0869	0.0864	0.0442	0.0192	
16		259.80	206.02	0.0882	0.0928	0.0553	0.0170	
17	40 25 20 49 122 58 38 95	287.53	221.52	0.0902	0.0937	0.0652	0.0237	
18	88 70 75 106 130 131 32	324.80	242.35	0.0926	0.0947	0.0765	0.0316	
19		455.18	346.19	0.1040	0.1045	0.0976	0.0457	
20		525.53	423.69	0.1087	0.1055	0.1058	0.0506	
21		670.46	676.39	0.1199	0.1108	0.1152	0.0635	
22	38 24 10 31 47 58 6 3 90	722.50	863.33	0.1228	0.1200	0.1092	0.0688	
23	70 95 101 62 105 19	556.12	626.61	0.1085	0.1024	0.0983	0.0568	
24		442.76	472.04	0.0975	0.0940	0.0894	0.0474	
		8947.80	7867.86	2.2894	2.2529	1.8041	0.8341	
Total energy loss (kWh), load balancing index, maximum node voltage deviation, and numbers of switching operations during 24 hours								

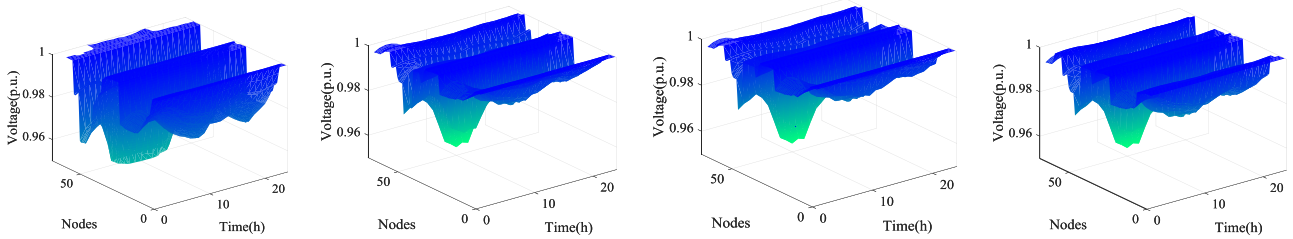

(a) Original system (b) CDBAS algorithm (c) PSO algorithm (d) BAS algorithm

FIGURE 11. Voltage profile of the 69 bus networks with DG for 24 hours.

total maximum node voltage deviation of 1.1049 in Case 6 are both slightly better than the total power loss of 7867.86 kWh, the load balancing of 2.2529 and the total maximum node voltage deviation of 0.8341 in Case 5 over 24 hours. Due to the limitation of installation location and capacity of the DG, the reconstruction results of Case 6 can only ensure that

TABLE 18. Real-time results of Cases 6 of the 118-bus system over 24 hours.

Hour	Open switches	Active power loss (kW)	Load balancing index (p.u)	Maximum node voltage deviation index (p.u)	Numbers of switching operations
1	23 25 3 49 47 29 38 90 66 85 96 81 101 114 27	173.17	0.0576	0.0063	–
2	28 25 20 53 47 57 4 63 88 72 73 102 130 114 132	163.07	0.0520	0.0223	
3	3 25 22 50 46 57 5 62 89 77 97 81 99 101 34	157.38	0.0480	0.0228	
4	41 25 19 47 30 61 38 125 66 73 75 78 85 116 9	169.48	0.0711	0.0219	
5	45 19 6 50 32 59 37 125 67 86 96 78 85 115 10	201.03	0.0692	0.0234	
6	25 12 22 121 48 61 39 89 70 87 73 129 78 116 32	228.54	0.0798	0.0384	
7	25 20 120 49 56 123 39 95 70 74 76 78 85 115 9	272.93	0.0900	0.0374	
8	24 14 17 121 31 58 37 54 90 72 75 82 85 116 132	402.87	0.1036	0.0721	
9	41 25 22 121 47 58 6 56 67 73 95 79 85 105 34	423.16	0.1105	0.0656	
10	43 17 6 40 47 57 8 63 126 74 96 81 99 116 28	203.24	0.0592	0.0248	
11	39 119 23 52 48 29 28 64 69 77 76 82 99 106 24	401.85	0.0929	0.0246	
12	25 119 6 42 48 54 8 63 90 70 128 82 99 109 29	233.97	0.0692	0.0207	
13	25 13 21 49 47 58 39 95 66 86 74 81 85 114 31	300.30	0.0969	0.0322	
14	26 13 20 41 47 58 39 95 67 73 96 79 85 116 132	244.06	0.0843	0.0182	
15	43 25 23 121 47 60 7 125 70 87 95 79 78 113 31	271.29	0.0908	0.0249	
16	44 12 4 50 48 60 37 95 66 127 73 80 85 106 21	274.98	0.0879	0.0302	
17	26 11 18 41 47 60 38 125 126 70 98 82 103 117 32	314.15	0.0917	0.0259	
18	9 26 120 50 47 55 7 64 67 78 74 105 101 109 29	232.67	0.0721	0.0211	
19	25 15 21 121 46 56 6 95 126 73 75 82 103 108 31	372.71	0.0970	0.0441	
20	3 25 22 50 47 35 28 63 88 78 76 100 85 107 32	417.74	0.0900	0.0357	
21	42 24 20 47 56 36 38 62 66 78 74 80 99 103 10	429.03	0.1043	0.0264	
22	44 24 17 41 48 35 27 63 65 73 98 82 103 117 3	114.91	0.0392	0.0679	
23	42 25 3 49 48 57 39 89 67 78 76 129 99 103 33	275.87	0.0756	0.0696	
24	23 119 6 52 46 57 124 62 72 78 74 79 104 113 29	175.68	0.0564	0.0059	
Total energy loss (kWh), load balancing index, maximum node voltage deviation, and numbers of switching operations during 24 hours		6454.10	1.8900	1.1049	

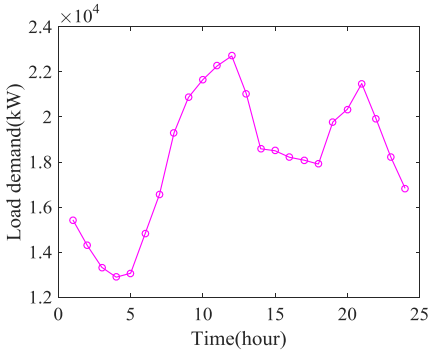

FIGURE 12. Load demand curve of different load types over 24 hours.

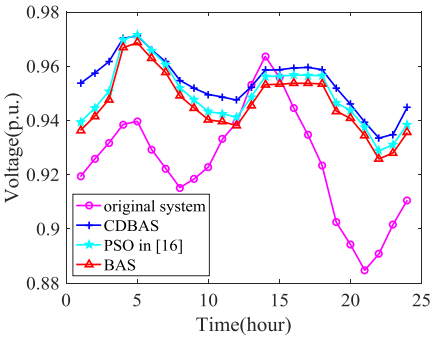

FIGURE 13. Voltage profile of the 118 bus networks with DG for 24 hours.

the voltage at a certain time meets the constraint condition. However, the reconfiguration results of Case 5 can satisfy the voltage constraint in the whole reconstruction period, so that the total active power loss increase slightly, the load balancing decreases slightly, and the voltage deviation increases slightly with the variation of load and DG.

IX. CONCLUSION

Considering multiobjective network reconfiguration based on variations in load and distributed generation (DG) for distribution systems has a strong effect on ensuring the safe and economical operation of a power system. In this study, minimizing the sum of active power loss, the load balancing index and the maximum node voltage deviation are considered as the objectives, and then the optimization problem of the layering relationship between each index and the number of switching operations is solved using grey target decision-making technology. Beetle Antennae Search (BAS) has the advantages of efficient optimization and small computation; however, it often converges to local optima. The improved Chaotic Disturbed Beetle Antennae Search (CDBAS) algorithm, which guarantees efficient calculation, is used to optimize multiobjective network reconfiguration in distribution systems.

Here, the proposed method can achieve the optimization of each objective in other words, it is valid and feasible through simulation in the modified IEEE 33, 69 and 118-bus system with variation of load and DG over 24 hours. Finally, compared with other methods in terms of speed and accuracy, the CDBAS method is accurate and converges very rapidly, so it can be used to solve optimization problems in multiple fields, such as the distribution network-planning schemes

considering load change, multi-source system schedules, and optimal storage allocations. Additionally, the proposed methodology can be applied to problems in which the objective functions are differentiable, non-differentiable, convex and non-convex with continuous and discrete variables.

REFERENCES

[1] J. Shukla, B. Das, and V. Pant, "Stability constrained optimal distribution system reconfiguration considering uncertainties in correlated loads and distributed generations," *Int. J. Elect. Power Energy Syst.*, vol. 99, no. 1, pp. 121–133, Jan. 2018, doi: 10.1016/j.ijepes.2018.01.010.

[2] R. S. Rao, S. V. L. Narasimham, M. R. Raju, and A. S. Rao, "Optimal network reconfiguration of large-scale distribution system using harmony search algorithm," *IEEE Trans. Power Syst.*, vol. 26, no. 3, pp. 1080–1088, Aug. 2011.

[3] D. S. Rani, "Multi-objective invasive wed optimization—An application to optimal network reconfiguration in radial distribution systems," *Int. J. Elect. Power Energy Syst.*, vol. 73, pp. 932–942, Jul. 2015, doi: 10.1016/j.ijepes.2015.06.020.

[4] T. T. Nguyen, "Multi-objective electric distribution network reconfiguration solution using runner-root algorithm," *Appl. Soft Comput.*, vol. 52, pp. 93–108, Mar. 2017, doi: 10.1016/j.asoc.2016.12.018.

[5] A. Ahuja, S. Das, and A. Pahwa, "An AIS-ACO hybrid approach for multi-objective distribution system reconfiguration," in *Proc. 21st IEEE Power Energy Soc. Gen. Meeting Convers. Delivery Elect. Energy Century*, Pittsburgh, PA, USA, Jul. 2008, p. 1.

[6] T. Niknam, "A new hybrid algorithm for multi-objective distribution feeder reconfiguration," *Cybern. Syst.*, vol. 40, no. 6, pp. 508–527, Jul. 2009.

[7] M.-S. Tsai and F.-Y. Hsu, "Application of grey correlation analysis in evolutionary programming for distribution system feeder reconfiguration," *IEEE Trans. Power Syst.*, vol. 25, no. 2, pp. 1126–1133, May 2010.

[8] A. Swarnkar, N. Gupta, and K. R. Niazi, "Reconfiguration of radial distribution systems with fuzzy multi-objective approach using adaptive particle swarm optimization," in *Proc. IEEE PES Gen. Meeting*, Providence, RI, USA, May 2010, pp. 1–8.

[9] H. Sun and Y. Ding, "Network reconfiguration of distribution system using fuzzy preferences multi-objective approach," in *Proc. 2nd Int. Asia Conf. Inform. Control, Automat. Robot.*, Mar. 2010, pp. 93–96.

[10] M. Sedighizadeh, S. Ahmadi, and M. Sarvi, "An efficient hybrid big bang–big crunch algorithm for multi-objective reconfiguration of balanced and unbalanced distribution systems in fuzzy framework," *Elect. Power Distrib. Netw.*, vol. 41, no. 1, pp. 75–99, 2013.

[11] A. Kavousi-Fard, T. Niknam, and M. Fotuhi-Firuzabad, "A novel stochastic framework based on cloud theory and θ-modified bat algorithm to solve the distribution feeder reconfiguration," *IEEE Trans. Smart Grid*, vol. 7, no. 2, pp. 740–750, Mar. 2016.

[12] A. Jafari, H. G. Ganjehlou, F. B. Darbandi, B. Mohammdi-Ivatloo, and M. Abapour, "Dynamic and multi-objective reconfiguration of distribution network using a novel hybrid algorithm with parallel processing capability," *Appl. Soft Comput.*, vol. 90, Apr. 2020, Art. no. 106146, doi: 10.1016/j.asoc.2020.106146.

[13] M. A. Muhammad, H. Mokhlis, K. Naidu, J. F. Franco, H. A. Illias, and L. Wang, "Integrated database approach in multi-objective network reconfiguration for distribution system using discrete optimisation techniques," *IET Gener., Transmiss. Distrib.*, vol. 12, no. 4, pp. 976–986, Feb. 2018, doi: 10.1049/iet-gtd.2017.1134.

[14] A. R. Malekpour, T. Niknam, A. Pahwa, and A. K. Fard, "Multi-objective stochastic distribution feeder reconfiguration in systems with wind power generators and fuel cells using the point estimate method," *IEEE Trans. Power Syst.*, vol. 28, no. 2, pp. 1483–1492, May 2013.

[15] E. Mahboubi-Moghaddam, M. R. Narimani, M. H. Khooban, A. Azizivahed, and M. J. Sharifi, "Multi-objective distribution feeder reconfiguration to improve transient stability, and minimize power loss and operation cost using an enhanced evolutionary algorithm at the presence of distributed generations," *Int. J. Elect. Power Energy Syst.*, vol. 76, pp. 35–43, Mar. 2016, doi: 10.1016/j.ijepes.2015.09.007.

[16] R. Tuladha, J. Singh, and W. Ongsakul, "A multi-objective network reconfiguration of distribution network with solar and wind distributed generation using NSPSO," in *Proc. Int. Conf. Green Energy Sustain. Develop.*, Cape Town, South Africa, Dec. 2014, pp. 1–7.

[17] J. Liu, H. Z. Cheng, and J. Xiao, "A multi-objective reconfiguration strategy for smart distribution network considering N-1 security criterion," *Autom. Electr. power Syst.*, vol. 40, no. 7, pp. 9–15, 2016.

[18] A. Azizivahed, H. Narimani, E. Naderi, M. Fathi, and M. R. Narimani, "A hybrid evolutionary algorithm for secure multi-objective distribution feeder reconfiguration," *Energy*, vol. 138, pp. 355–373, Dec. 2017, doi: 10.1016/j.energy.2017.07.102.

[19] C. Gerez, L. I. Silva, E. A. Belati, A. J. Sguarezi Filho, and E. C. M. Costa, "Distribution network reconfiguration using selective firefly algorithm and a load flow analysis criterion for reducing the search space," *IEEE Access*, vol. 7, pp. 67874–67888, 2019.

[20] H. Sun, C. Peng, and X. Yuan, "Multi-objective dynamic distribution network reconfiguration considering switching frequency," *Electr. Power Automat. Equip.*, vol. 34, no. 9, pp. 41–46, 2014, doi: 10.3969/j.issn.1006-6047.2014.09.007.

[21] S. Cheng and Z. Li, "Multi-objective network reconfiguration considering V2G of electric vehicles in distribution system with renewable energy," *Energy Procedia*, vol. 158, pp. 278–283, Oct. 2019, doi: 10.1016/j.egypro.2019.01.089.

[22] E. kianmehr, S. Nikkhah, and A. Rabiee, "Multi-objective stochastic model for joint optimal allocation of DG units and network reconfiguration from DG owner's and DisCo's perspectives," *Renew. Energy*, vol. 132, pp. 471–485, May 2019, doi: 10.1016/j.renene.2018.08.032.

[23] M. A. T. G. Jahani, P. Nazarian, A. Safari, and M. R. Haghifam, "Multi-objective optimization model for optimal reconfiguration of distribution networks with demand response services," *Sustain. Cities Soc.*, vol. 47, May 2019, Art. no. 101514, doi: 10.1016/j.scs.2019.101514.

[24] M. Esmaeili, M. Sedighizadeh, and M. Esmaili, "Multi-objective optimal reconfiguration and DG (distributed generation) power allocation in distribution networks using big bang-big Crunch algorithm considering load uncertainty," *Energy*, vol. 103, pp. 86–99, Oct. 2016, doi: 10.1016/j.energy.2016.02.152.

[25] X. Kong, C. Yong, C. Wang, P. Li, L. Yu, and Y. Chen, "Multi-objective power supply capacity evaluation method for active distribution network in power market environment," *Int. J. Electr. Power Energy Syst.*, vol. 115, May 2020, Art. no. 105467, doi: 10.1016/j.ijepes.2019.105467.

[26] C. Xingang, T. Hao, Y. Bing, L. Changxin, and C. Xiaoqing, "Multi-objective distribution network reconfiguration based on deep learning algorithm," in *Proc. IEEE Int. Conf. High Voltage Eng. Appl. (ICHVE)*, Athens, Greece, Sep. 2018, pp. 1–4.

[27] I. A. Quadri, S. Bhowmick, and D. Joshi, "Multi-objective approach to maximise loadability of distribution networks by simultaneous reconfiguration and allocation of distributed energy resources," *IET Gener., Transmiss. Distrib.*, vol. 12, no. 21, pp. 5700–5712, Nov. 2018.

[28] X. Jiang and S. Li, "BAS: Beetle antennae search algorithm for optimization problems," Oct. 2017, *arXiv:1710.10724*. [Online]. Available: https://arxiv.org/abs/1710.10724

[29] Z. Zhu, Z. Zhang, W. Man, and X. Tong, "A new beetle antennae search algorithm for multi-objective energy management in microgrid," in *Proc. 13th IEEE Conf. Ind. Electron. Appl. (ICIEA)*, Wuhan, China, May 2018, pp. 1599–1603.

[30] Y. G. Dong and S. F. Liu, *Grey System Theory and its Application*. BeiJing, China: Science Press, 2014, pp. 256–261.

[31] H. Z. Zhou, F. Tang, and D. Liu, "Active distribution network dynamic reconfiguration and DG dynamic control strategy considering time-variant load," *Power Syst. Technol.*, vol. 40., no. 8, 2016, pp. 2423–2429.

[32] T. L. Zang, Z. Y. He, and D. Y. Ye, "Distribution network service restoration based on interval number grey relation decision-making considering load change," *Power Syst. Protection Control*, vol. 41, no. 3, pp. 38–43, Feb. 2013.

[33] N. Xiong and H. Z. Cheng, "Switch group-based tabu algorithm applied in distribution network dynamic reconfiguration," *Automat. Electr. Power Syst.*, vol. 32 no. 11, pp. 56–60, 2008.

[34] H. C. Yi, B. D. Zhang, and H. Y. Wang, "Distribution network dynamic reconfiguration method for improving distribution network's ability of accepting DG," *Power Syst. Technol.*, vol. 40, no. 5, 2016, pp. 1431–1436.

[35] Q. H. Zuo, X. Li, L. Yang, Y. Huang, M. Wang, and J. Huang, "Multi-objective distribution network dynamic reconfiguration and DG control considering time variation of load and DG," *High Voltage Eng.*, vol. 45, pp. 873–881, Apr. 2019.

[36] M. A. Samman, H. Mokhlis, N. N. Mansor, H. Mohamad, H. Suyono, and N. M. Sapari, "Fast optimal network reconfiguration with guided initialization based on a simplified network approach," *IEEE Access*, vol. 8, pp. 11948–11963, 2020.
[37] S. K. Injeti and N. P. Kumar, "A novel approach to identify optimal access point and capacity of multiple DGs in a small, medium and large scale radial distribution systems," *Int. J. Electr. Power Energy Syst.*, vol. 45, no. 1, pp. 142–151, 2013, doi: 10.1016/j.ijepes.2012.08.043.

JIE WANG received the B.E. and M.E. degrees in electric power systems and automation from Xinjiang University, Urumqi, China, in 2014 and 2018, respectively. She is currently pursuing the Ph.D. degree with the Engineering Research Center of Renewable Energy Power Generation and Grid-connected Control, Ministry of Education, Xinjiang University. Her current research interests include the control of renewable energy power generation and smart grid technology.

WEIQING WANG received the B.E. degree in electric power systems and automation from the Xinjiang Institute of Technology, Urumqi, China, in 1983, and the M.E. degree in electric power systems and automation from Zhejiang University, Hangzhou, China, in 1990. He is currently a Professor with the Engineering Research Center of Renewable Energy Power Generation and Grid-connected Control, Ministry of Education, Xinjiang University. His current research interests include the control of renewable energy power generation and smart grid technology.

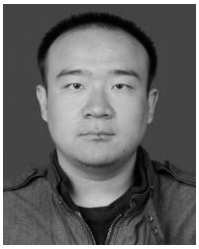

ZHI YUAN received the B.E. degree in electric power systems and automation from North China Electrical Power University, Baoding, China, in 2007, and the M.E. and Ph.D. degrees in electric power systems and automation from Xinjiang University, Urumqi, China, in 2012 and 2016, respectively. He is currently an Associate Professor with the Engineering Research Center of Renewable Energy Power Generation and Grid-Connected Control, Ministry of Education, Xinjiang University. His current research interests include the control of renewable energy power generation and smart grid technology.

HAIYUN WANG received the B.E. degree in electric power systems and automation from Xinjiang University, Urumqi, China, in 1995, and the M.E. degree in electrical engineering from the Dalian University of Technology, Liaoning, China, in 1999. She is currently a Professor with the Engineering Research Center of Renewable Energy Power Generation and Grid-Connected Control, Ministry of Education, Xinjiang University. Her current research interests include the control of renewable energy power generation and smart grid technology.

JIAHUI WU received the B.E. degree in chemical technology and automation from the Beijing University of Chemical Technology, Beijing, China, in 2011, and the Ph.D. degree in electric power systems and automation from Xinjiang University, Urumqi, China, in 2018. She is currently an Associate Professor with the Engineering Research Center of Renewable Energy Power Generation and Grid-Connected Control, Ministry of Education, Xinjiang University. Her current research interests include the control of renewable energy power generation and smart grid technology.